ACI STRUCTURAL JOURNAL TECHNICAL PAPER

Title no. 103-S55

Behavior and Capacity of Headed Reinforcement

by M. Keith Thompson, James O. Jirsa, and John E. Breen

Results from two studies of headed reinforcement have been combined to develop design recommendations for headed reinforcement. Important aspects of headed bar anchorage are summarized, and a model for determining the anchorage capacity of headed reinforcement is presented. The model includes two components that contribute to the total bar stress, head bearing, and bond, each calculated separately. The proposed model is compared to data from previous headed bar studies. Proper use of the model and areas for additional study are discussed.

Keywords: anchorage; lap splice; reinforcement.

INTRODUCTION

The Texas Department of Transportation (TxDOT) funded a program to study the feasibility of headed reinforcement in bridge structures. Under this project, two basic anchorage conditions for headed reinforcement were studied: 1) anchorage at compression-compression-tension (CCT) nodes; and 2) anchorage in lap splices. Results from these test programs have provided the basis for a general design approach for ensuring adequate detailing of headed reinforcement.

RESEARCH SIGNIFICANCE

Data from test programs of CCT nodes and lap splices are compared. Similarities in observed behavior support the proposal of a single design model for headed bar anchorage. Recommendations for calculating the anchorage capacity of headed reinforcement have been developed by combining the results of the two studies. These recommendations were used to analyze results from previous studies of headed reinforcement and the understanding of previous test results was enhanced.

TEST PROGRAMS

CCT nodes

A typical CCT node specimen is shown in Fig. 1. The basic CCT node configuration was unconfined (no local reinforcement aside from the tie bar) and anchored only a single tie bar, thus reducing the number of parameters influencing behavior of the node. The major variables of the test program included head size (indicated by relative head area, A_{nh}/A_b = 0.0 to 10.4), bar size (25 or 36 mm diameter bars), and strut angle (30, 45, or 55 degrees). The test program also included a few companion tests with hooked bars or stirrup confinement. Further details of this test program are documented in References 1 and 2.

Lap splices

A typical lap splice specimen is shown in Fig. 2. As with the CCT nodes, the lap splice configuration was kept simple in order to reduce the number of influencing parameters. Lap zones in most specimens were unconfined and the basic arrangement of the lapped bars was varied little from test to test. The main variables of the test program were head size (A_{nh}/A_b = 0.0 to 4.7) and splice length (L_s/d_b = 3.0 to 14.0). Additional parameters, which were studied in only a few tests, included contact versus non-contact lap arrangements, bar spacing ($6d_b$ or $10d_b$), and confinement details. Further details of this test program are documented in Reference 3.

In both test programs, three basic head types were used, representing the variety in headed reinforcement that was commercially available at the time of testing. The three basic head types are shown in Fig. 3. Within the scope of the test programs, there was little observed difference in behavior

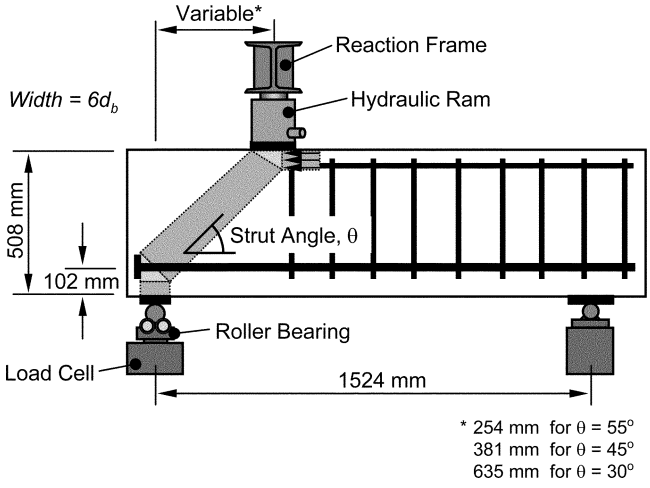

Fig. 1—Typical CCT node test.

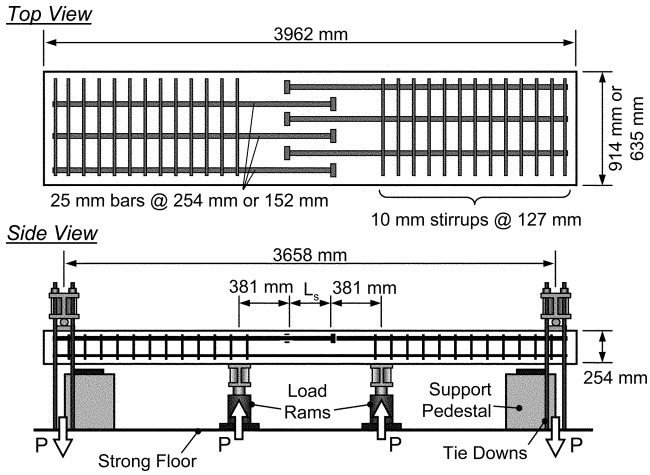

Fig. 2—Typical lap splice test.

ACI Structural Journal, V. 103, No. 4, July-August 2006.
MS No. 04-358 received November 1, 2004, and reviewed under Institute publication policies. Pertinent discussion including author's closure, if any, will be published in the May-June 2007 *ACI Structural Journal* if the discussion is received by January 1, 2007.

ACI member **M. Keith Thompson** *is an Assistant Professor at the University of Wisconsin-Platteville, Platteville, Wis. He received his BS from North Carolina State University, Raleigh, N.C., and his MS and PhD from the University of Texas at Austin, Austin, Tex. His research interests include anchorage of reinforcement and strut-and-tie modeling.*

James O. Jirsa, *FACI, holds the Janet S. Cockrell Centennial Chair in Engineering at the University of Texas at Austin. He is a Past President of ACI, a member of the ACI Board of Direction, and a Past Chair of the Technical Activities Committee. He is a member of ACI Committees 318, Structural Concrete Building Code; 408, Bond and Development of Reinforcement; and is a member and Chair of ACI Subcommittee 318-F, New Materials, Products, and Ideas.*

ACI Honorary Member **John E. Breen** *holds the Nasser I. Al-Rashid Chair in Civil Engineering at the University of Texas at Austin. He is a member and Past Chair of ACI Committee 318, Structural Concrete Building Code; is a member of ACI Committee 355, Anchorage to Concrete; ACI Subcommittees 318-B, Reinforcement and Development, and 318-E, Shear and Torsion; and is a Past Chair of the Technical Activities Committee.*

between head types when equal bearing areas were provided. The recommendations contained in this paper are intended to apply to each of these head types.

TEST RESULTS

Stages of anchorage

Headed bar anchorage is provided by a combination of head bearing and bond. Initial anchorage is carried primarily by bond. As additional stress is applied to the bar, bond achieves peak capacity and begins to decline. As the process of bond deterioration occurs, bar anchorage is transferred to the head, causing a rise in head bearing. The anchorage capacity at failure is provided by a combination of peak head bearing and reduced bond. This pattern of behavior was observed in both CCT node and lap splice tests (Fig. 4). Using this understanding of headed bar anchorage, a model for anchorage capacity was developed based on separate models for the head bearing and bond components.

Model for bearing capacity

The proposed model for head bearing capacity is based on existing ACI[4] code equations for bearing strength and side blowout capacity. A database including more than 500 tests of anchor bolts, headed bars, and rigid bearing plates was used to create the model. Development of the model is documented in Reference 2. The equations used in the model are listed below

$$\text{Bearing pressure, } \frac{N}{A_{nh}} = 0.9 \cdot n_{5\%} \cdot f_c' \left(\frac{2c}{\sqrt{A_{nh}}} \right) \Psi \qquad (1)$$

$$\text{where } \Psi = 0.6 + 0.4\left(\frac{c_2}{c}\right) \le 2.0 \qquad (2)$$

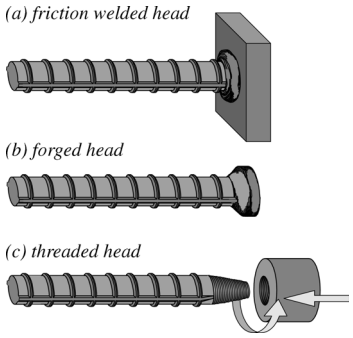

Fig. 3—Head types.

The $n_{5\%}$ term adjusts the model such that only 5% of tests from the database had a capacity less than that calculated by the model. A value of 0.7 is recommended. Without the $n_{5\%}$ term, the model calculates the mean capacity of the test data. The model does not apply if the anchorage length L_a becomes too short. A minimum anchorage length of $6d_b$ is suggested.[3]

Equation (1) can be reformatted to calculate the bar stress provided by the head $f_{s,head}$

$$\text{Bar stress, } f_{s,head} = \frac{N}{A_b} 0.9 \cdot n_{5\%} \cdot f_c' \left(\frac{2c}{\sqrt{A_{nh}}} \right) \Psi \cdot \frac{A_{nh}}{A_b}$$

$$= n_{5\%} \cdot f_c' \cdot \Psi \cdot 1.8\left(c \cdot \frac{1}{\sqrt{A_b}} \right) \cdot \sqrt{\frac{A_{nh}}{A_b}}$$

Substituting $\sqrt{A_b} \cong 0.9 d_b$

$$f_{s,head} = n_{5\%} \cdot 2 \cdot f_c' \cdot \left(\frac{c}{d_b} \right) \cdot \sqrt{\frac{A_{nh}}{A_b}} \cdot \Psi \qquad (3)$$

This equation provides the bar stress from the head in terms of three non-dimensional parameters: 1) relative cover dimension (c/d_b); 2) relative head area (A_{nh}/A_b); and 3) the radial disturbance factor (Ψ). A radial disturbance factor of 1.0 can be used conservatively in calculations of $f_{s,head}$. Measured and calculated values of $f_{s,head}$ are presented for the CCT node and lap splice tests in Table 1.

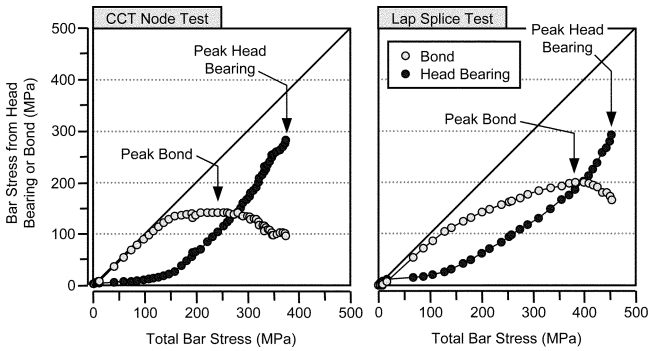

Fig. 4—Bond and head bearing anchorage components.

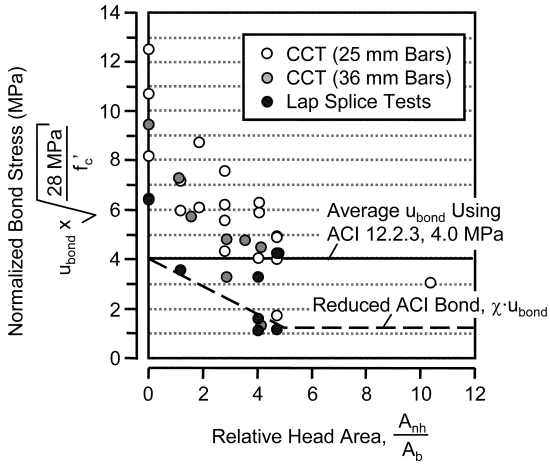

Fig. 5—Reduction in bond with increasing head size.

Model for bond capacity

The existing ACI equation for development length was used as a basis for computing the bar stress provided by bond. To account for the reduction in bond stress that occurs from addition of a head to the bar, a factor was developed to adjust the ACI development-length-based bar stress. This head size reduction factor is based on a database of 28 CCT node tests and eight lap splice tests (data are presented in Table 2). Failure bond values from the database are plotted in Fig. 5 (the data have been normalized with respect to a concrete strength of 28 MPa by the square root of the ratio 28 MPa/f_c'). The following trend was approximated for the reduction in bond as a function of head size

$$\text{Reduction factor, } \chi = 1 - 0.7\left(\frac{A_{nh}/A_b}{5}\right) \geq 0.3 \qquad (4)$$

The average bond calculated using the product of the ACI development length equation and the factor given in Eq. (4) are also plotted in Fig. 5. Much of the measured data plotted significantly higher than the values calculated using the proposed model for bond stress.

Table 1—Summary of results for head bearing component

	Head dimensions, mm	d_b, mm	Variables of head model				$f_{s,\,head}$, MPa		Measured/ calculated
			A_{nh}/A_b	c/d_b	c_2/d_b	f_c', MPa	Measured*	Calculated	
CCT Nodes	No head	25	0.00	3.0	4.0	27	—	0	—
	d_h = 38	25	1.18	3.0	4.0	27	261	123	1.88
	38 x 38	25	1.85	3.0	4.0	27	288	174	1.65
	51 x 38	25	2.80	3.0	4.0	27	262	214	1.22
	38 x 51	25	2.80	3.0	4.0	27	298	214	1.39
	d_h = 57	25	4.04	3.0	4.0	21	219	205	1.07
	51 x 51	25	4.06	3.0	4.0	21	240	205	1.17
	76 x 38	25	4.70	3.0	4.0	21	359	221	1.63
	38 x 76	25	4.70	3.0	4.0	27	335	277	1.21
	No head	25	0.00	3.0	4.0	28	—	0	—
	d_h = 38	25	1.18	3.0	4.0	28	128	111	1.16
	38 x 38	25	1.85	3.0	4.0	28	183	179	1.03
	38 x 38	25	1.85	3.0	4.0	21	204	138	1.48
	51 x 38	25	2.80	3.0	4.0	21	259	170	1.52
	38 x 51	25	2.80	3.0	4.0	27	339	214	1.58
	51 x 51	25	4.06	3.0	4.0	21	304	205	1.48
	76 x 38	25	4.70	3.0	4.0	21	370	221	1.68
	38 x 76	25	4.70	3.0	4.0	27	336	277	1.21
	76 x 76	25	10.39	3.0	4.0	21	—	328	—
	76 x 76	25	10.39	3.0	4.0	26	377	402	0.94
	No head	25	0.00	3.0	4.0	28	—	0	—
	d_h = 38	25	1.18	3.0	4.0	28	206	150	1.38
	No head	36	0.00	2.8	3.0	28	—	0	—
	d_h = 52	36	1.10	2.8	3.0	28	147	120	1.23
	51 x 51	36	1.56	2.8	3.0	28	208	142	1.46
	76 x 51	36	2.85	2.8	3.0	28	209	192	1.08
	51 x 76	36	2.85	2.8	3.0	28	282	192	1.47
	d_h = 76	36	3.53	2.8	3.0	28	254	204	1.25
	102 x 51	36	4.13	2.8	3.0	28	390	232	1.68
	51 x 102	36	4.13	2.8	3.0	28	269	220	1.22
	76 x76	36	4.77	2.8	3.0	28	274	237	1.16
Lap splices	No head	25	0.00	2.5	2.5	28	—	0	—
	No head	25	0.00	2.5	2.5	29	—	0	—
	d_h = 38	25	1.18	2.5	2.5	28	97	105	0.92
	38 x 76	25	4.70	2.5	2.5	28	272	209	1.30
	d_h = 57	25	4.04	2.5	2.5	28	279	194	1.44
	38 x 76	25	4.70	2.5	2.5	29	292	199	1.47
	d_h = 57	25	4.04	2.5	2.5	26	287	199	1.44
	d_h = 57	25	4.04	2.5	2.5	24	270	175	1.55
	d_h = 57	25	4.04	2.5	5.0†	24	375	244	1.54

Note: — = Data not available or not applicable.

*Head capacity measured at $1d_b$ from face of head for CCT node tests and $2d_b$ from face of head for lap splice tests. No data is provided for non-headed bars.

†Sheath used to prevent bond.

Under the proposed model, the bar stress contributed from bond is calculated using the ratio of available anchorage length L_a to development length L_d, assuming that the distribution of bar stress is linear over L_d (refer to Fig. 6). This produces a baseline stress, $f_{s,bond} = f_y(L_a/L_d)$. If a head is attached to the bar, then $f_{s,bond}$ must be reduced by the reduction factor

$$f_{s,bond} = \chi \cdot \left(\frac{L_a}{L_d}\right) \cdot f_y \quad (5)$$

Measured and calculated values of $f_{s,bond}$ are presented for the CCT node and lap splice tests in Table 2. The recommended procedure produced conservative results for all but two of the tests. It should be noted that the equation for the reduction factor is based on limited data and some subjective judgment of data trends. This approach may not recognize all of the factors influencing bond in headed reinforcement and is not necessarily an optimal fit of the data. This approach is simple, however, and provides a conservative calculation when compared with the majority of the data, and recognizes the dominant trend of the data.

Table 2—Summary of results for bond component

	Head dimensions, mm	d_b, mm	Variables of bond model				$f_{s,head}$, MPa		Measured/ calculated
			A_{nh}/A_b	L_d/d_b	L_a/L_b	f_c', MPa	Measured*	Calculated	
CCT Nodes	No head	25	0.00	7.0	0.24	27	346	100	3.44
	d_h = 38	25	1.18	7.0	0.24	27	165	84	1.97
	38 x 38	25	1.85	7.0	0.24	27	168	74	2.26
	51 x 38	25	2.80	7.0	0.24	27	209	61	3.43
	38 x 51	25	2.80	7.0	0.24	27	154	61	2.51
	d_h = 57	25	4.04	7.0	0.22	21	100	39	2.58
	51 x 51	25	4.06	7.0	0.22	21	146	39	3.77
	76 x 38	25	4.70	7.0	0.22	21	99	31	3.24
	38 x 76	25	4.70	7.0	0.24	27	137	34	3.97
	No head	25	0.00	7.0	0.25	28	299	102	2.94
	d_h = 38	25	1.18	7.0	0.22	28	—	75	—
	38 x 38	25	1.85	7.0	0.25	28	—	75	—
	38 x 38	25	1.85	7.0	0.22	21	216	66	3.25
	51 x 38	25	2.80	7.0	0.22	21	154	54	2.82
	38 x 51	25	2.80	7.0	0.24	27	120	61	1.96
	51 x 51	25	4.06	7.0	0.22	21	155	39	4.02
	76 x 38	25	4.70	7.0	0.22	21	43	31	1.40
	38 x 76	25	4.70	7.0	0.24	27	135	34	3.94
	76 x 76	25	10.39	7.0	0.22	21	—	27	—
	76 x 76	25	10.39	7.0	0.24	26	83	30	2.79
	No head	25	0.00	7.0	0.25	28	235	104	2.25
	d_h = 38	25	1.18	7.0	0.25	28	206	87	2.37
	No head	36	0.00	7.0	0.25	28	268	103	2.60
	d_h = 52	36	1.10	7.0	0.25	28	207	87	2.37
	51 x 51	36	1.56	7.0	0.25	28	162	81	2.01
	76 x 51	36	2.85	7.0	0.25	28	137	62	2.21
	51 x 76	36	2.85	7.0	0.25	28	93	62	1.51
	d_h = 76	36	3.53	7.0	0.24	28	133	51	2.61
	102 x 51	36	4.13	7.0	0.25	28	37	43	0.85
	51 x 102	36	4.13	7.0	0.24	28	124	42	2.93
	76 x76	36	4.77	7.0	0.24	28	118	33	3.54
Lap splices	No head	25	0.00	6.0	0.21	28	154	87	1.77
	No head	25	0.00	10.0	0.36	29	262	147	1.78
	d_h = 38	25	1.18	6.0	0.21	28	85	73	1.78
	38 x 76	25	4.70	6.0	0.21	28	28	30	0.93
	d_h = 57	25	4.04	6.0	0.21	28	27	38	0.72
	38 x 76	25	4.70	10.0	0.34	29	165	48	3.41
	d_h = 57	25	4.04	10.0	0.36	26	65	64	1.01
	d_h = 57	25	4.04	12.0	0.40	24	151	72	2.10
	d_h = 57	25	4.04	—†	—	24	—	0	—

Note: — = Data not available or not applicable.
*Full anchorage length was used to determine bond for nonheaded bars. For headed bars, only anchorage length to the strain gauge nearest the head was used.
†Sheath used to prevent bond.

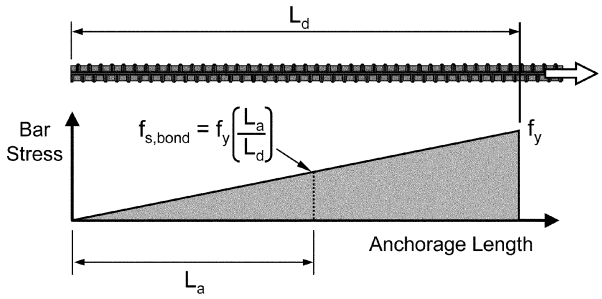

Fig. 6—Bar stress provided by anchorage length less than L_d.

Combination of bond and head bearing models

Summing the bond and head bearing models, total bar stress was calculated for the CCT node and lap splice tests (Table 3). A distribution plot of measured/calculated ratios is presented in Fig. 7. The combined models provided safe calculations of capacity for all tests. The average ratio of measured/calculated test values was a very conservative 1.7.

Comparison with other studies

Three previous studies provided an opportunity to compare the proposed model with additional test results:

Table 3—Summary of proposed model results

	Head dimensions, mm	Identifying variables				$f_{s,total}$, MPa		Measured/ calculated
		d_b, mm	A_{nh}/A_b	L_d/L_b	f_c', MPa	Measured*	Calculated	
CCT Nodes	No head	25	0.00	0.24	27	346	100	3.44
	d_h = 38	25	1.18	0.24	27	426	223	1.91
	38 x 38	25	1.85	0.24	27	456	249	1.84
	51 x 38	25	2.80	0.24	27	471	275	1.71
	38 x 51	25	2.80	0.24	27	451	275	1.64
	d_h = 57	25	4.04	0.22	21	319	243	1.31
	51 x 51	25	4.06	0.22	21	386	244	1.58
	76 x 38	25	4.70	0.22	21	458	251	1.82
	38 x 76	25	4.70	0.24	27	472	312	1.51
	No head	25	0.00	0.25	28	299	102	2.94
	d_h = 38	25	1.18	0.22	28	—	185	—
	38 x 38	25	1.85	0.25	28	—	254	—
	38 x 38	25	1.85	0.22	21	420	205	2.05
	51 x 38	25	2.80	0.22	21	413	225	1.84
	38 x 51	25	2.80	0.24	27	458	275	1.66
	51 x 51	25	4.06	0.22	21	459	244	1.88
	76 x 38	25	4.70	0.22	21	413	251	1.64
	38 x 76	25	4.70	0.24	27	471	312	1.51
	76 x 76	25	10.39	0.22	21	376	355	1.06
	76 x 76	25	10.39	0.24	26	460	432	1.07
	No head	25	0.00	0.25	28	235	104	2.25
	d_h = 38	25	1.18	0.25	28	412	237	1.74
	No head	36	0.00	0.25	28	268	103	2.60
	d_h = 52	36	1.10	0.25	28	354	207	1.71
	51 x 51	36	1.56	0.25	28	370	223	1.66
	76 x 51	36	2.85	0.25	28	345	254	1.36
	51 x 76	36	2.85	0.25	28	375	254	1.48
	d_h = 76	36	3.53	0.24	28	387	255	1.52
	102 x 51	36	4.13	0.25	28	427	275	1.55
	51 x 102	36	4.13	0.24	28	393	263	1.50
	76 x 76	36	4.77	0.24	28	392	270	1.45
Lap splices	No head	25	0.00	0.21	28	154	87	1.77
	No head	25	0.00	0.36	29	262	147	1.78
	d_h = 38	25	1.18	0.21	28	182	178	1.03
	38 x 76	25	4.70	0.21	28	300	239	1.25
	d_h = 57	25	4.04	0.21	28	306	232	1.32
	38 x 76	25	4.70	0.34	29	457	247	1.85
	d_h = 57	25	4.04	0.36	26	352	263	1.34
	d_h = 57	25	4.04	0.40	24	421	247	1.71
	d_h = 57	25	4.04	—†	24	375	244	1.54

Note: — = Data not available or not applicable.
*Strain gauge data at maximum stress point used to determine measured bar stress.
†Sheath used to prevent bond.

- Deeply embedded pullout tests at the University of Texas;[5,6]
- Beam-column joints at the University of Texas;[6] and
- Stub-beam pullout test at the University of Kansas.[7]

The basic parameters of these studies are summarized in Table 4.

Deep embedment pullout tests—The deep embedment pullout study tested headed bars embedded in mass concrete. Bars were pulled in direct tension and failed by side blowout. That study contained confined and unconfined test groups. Only those tests with both bond and head bearing components of anchorage were included in the comparison (tests in which a sheath prevented bond were excluded). All tests provided a ratio of embedment depth to cover greater than 5.0. The configuration of the tests allowed accurate determination of the anchorage length. The distribution of measured/calculated test values for the deep embedment pullout tests is plotted in Fig. 8. The model was conservative for all tests with an average measured/calculated value of 1.9. The proposed model was quite safe for this study.

Beam-column joint tests—The beam-column study tested pairs of headed bars used to anchor negative bending moment in beams at exterior column joints. Bars were pulled in tension and were reported to fail by side blowout or a shear-related rupture that resembled a combination of joint shear failure and concrete breakout. A typical test is shown in Fig. 9. Confinement in the form of vertical column bars and horizontal column stirrups was provided in varying amounts for all tests. The ratio of embedment depth to cover was between 3.2 and 7.3 for all tests. The configuration of the tests did not allow accurate determination of the anchorage length. Embedment depth was substituted for anchorage length in calculations of anchorage capacity. The average ratio of measured to calculated capacity was 1.0 with a range of 0.4 to 1.7. The proposed model was unconservative for approximately half the tests of this study, most likely a consequence from the substitution of embedment depth for anchorage length in bond calculations and from insufficient anchorage length to allow applicability of the head bearing model (a probable strut-and-tie model for one test is shown in Fig. 9. While the anchorage length could not be accurately determined, it must have been significantly less than the embedment depth). Measured/calculated ratios are plotted against embedment/cover ratio in Fig. 10.

Stub-beam pullout tests—The stub-beam study tested single headed bars used as anchorage for flexural reinforcement in the end regions of beam members. The stub-beam configuration allowed the bars to be tested in direct tension. Most tests included confinement in the form of vertical stirrups spaced evenly along the embedment depth of the bar. Bars tended to fail by spalling of the cover concrete. A typical test specimen

Table 4—Database for comparison to proposed model

Source	No. of data values	Ranges for variables			
		f_c', MPa	A_{nh}/A_b	c/d_b	L_d/d_b*
CCT node tests[3]	29	21 to 29	0.0 to 10.4	2.8 to 3.0	7.0
Lap splice tests[4]	8	25 to 28	0.0 to 4.7	2.5	6.0 to 12.0
Deep embedment[8,9]					
• Unconfined tests	15	21 to 27	4.7 to 9.0	1.8 to 2.4	7.6 to 18.3
• Confined tests	20	21 to 27	2.7 to 9.0	1.8 to 2.4	8.7 to 12.2
Beam column[9]					
• Side blowout failures	18	22 to 39	2.1 to 7.4	1.6 to 2.6	—
• Shear-related failures	14	23 to 40	2.1 to 7.4	1.7 to 2.6	—
Stub-beam pullout tests[10]					
• Unconfined tests	3	34	10.4	2.5	—
• Confined tests	13	34	10.4	2.5 to 3.5	—

*Anchorage length is unknown for beam-column pullout tests. However, embedment depth h_d is reported: h_d/d_b = 5.8 – 12.3 for beam-columns and h_d/d_b = 11 for pullout tests.

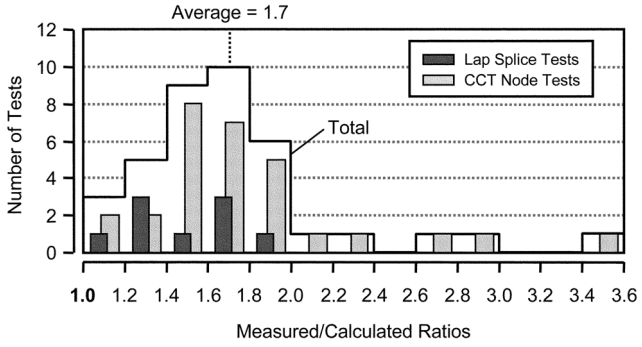

Fig. 7—Distribution plot of proposed model results for CCT and lap tests.

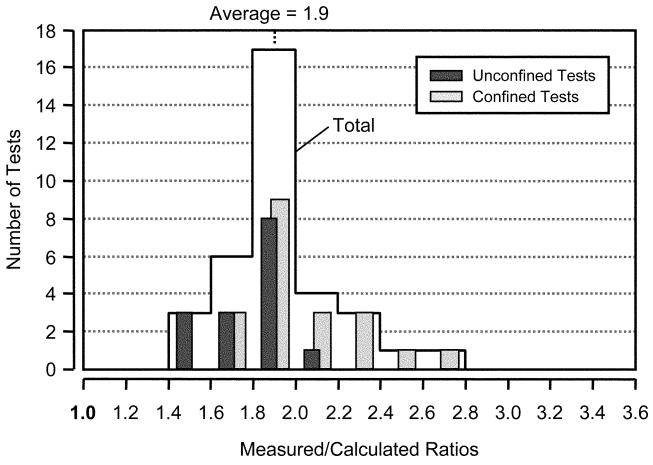

Fig. 8—Distribution plot of proposed model results for deeply embedded pullout tests.

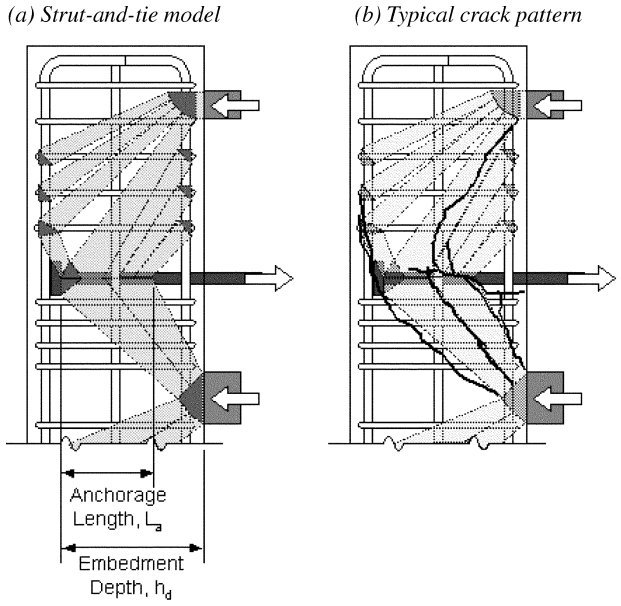

Fig. 9—Typical beam-column joint test with possible truss model.

with appearance at failure is shown in Fig. 11. The configuration of the test did not allow accurate determination of the anchorage length (the probable strut-and-tie model for a stub-beam test without stirrups is shown in Fig. 11. The anchorage length could not be calculated accurately, but must have been shorter than the embedment depth). The published embedment depth was substituted for anchorage length in calculations of anchorage capacity. The average ratio of measured to calculated capacity was 0.8 with a range of 0.5 to 0.9. The proposed model was unconservative for all tests of this study. Measured/calculated ratios are plotted against the embedment/cover ratio in Fig. 10.

DISCUSSION

Importance of anchorage length

The proposed model was inaccurate for the beam-column tests and stub-beam pullout tests because the anchorage length of the headed bars was not accounted for in the calculation of bond contribution or to determine the applicability of the model for head bearing. These results indicate the importance of anchorage length in the proposed model. Anchorage length L_a is measured from the bearing face of the head, the outside bend of a hook, or the end of a straight bar to the point of peak bar stress. When a strut-and-tie model is considered, the point of peak bar stress coincides approximately with the intersection of the tie bar with the leading edges of the compression struts anchored by the tie bar (the end of the extended nodal zone). Strut-and-tie modeling is the best approach to determine anchorage length.

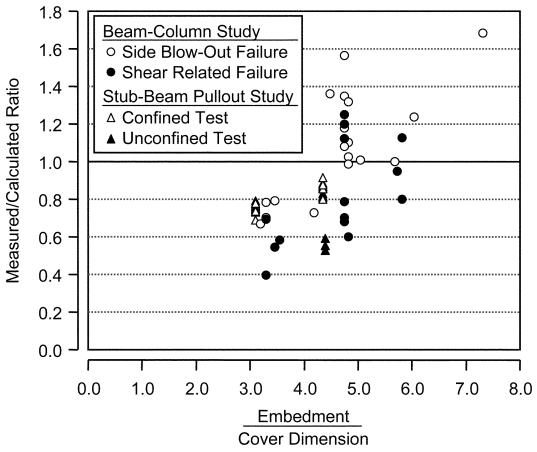

Fig. 10—Results from proposed model for beam-column and stub-beam studies.

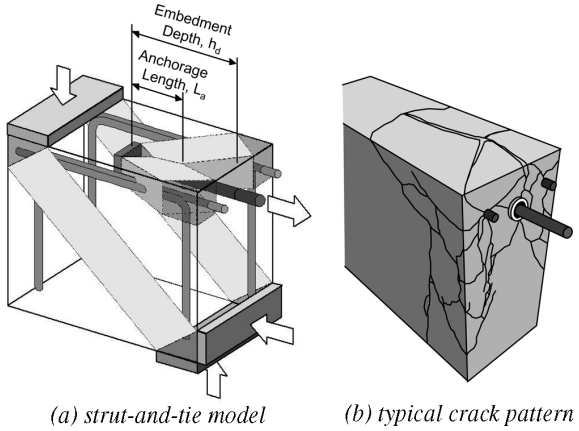

Fig. 11—Typical stub-beam test with possible truss model.

The recommendation of strut-and-tie modeling to determine anchorage length is a departure from conventional treatments of anchorage that use the splice length or embedment length to characterize capacity. The language and figures used in ACI 318-02, Chapter 12 ("Development and Splices of Reinforcement") recognize the critical section for development of reinforcement as that corresponding to maximum moment at a beam's midspan or at a joint. Thus, the development length expressions for straight bars and hooks are derived with a beam theory approach in mind. With a strut-and-tie approach, however, the strut-and-tie model will indicate, in many cases, that the critical section occurs at a different location. This is particularly true for joints.

As an example, consider the joint illustrated in Fig. R12.12(a) of ACI 318-02 (a representation of which is shown in Fig. 12(a)). The figure in the code shows the critical section to occur at the face of the column. The development length L_{dh} is compared to the embedment length of the bar into the column. Now consider a strut-and-tie model of the same joint as shown in Fig. 12(b). The tension in the hooked bar is balanced by compression Struts AB and AC (shown as dashed lines). Struts AB and AC occupy some height and width within the joint (Fig. 12(c)). Under the strut-and-tie model, the critical section of the hooked bar occurs where it intersects the leading edge of these struts. The resulting anchorage length is much shorter than the embedment length that is generally used to compare against development length.

Another example of the importance of this issue is provided by the failure of the original gravity-based support for the Sleipner A offshore oil platform.[8,9] The main report of the failure[9] concluded that failure was a result of inadequate design of the tricell joints formed at the intersections of adjacent caisson walls. Two primary flaws were cited: 1) errors in the finite element analysis used to calculate shear at the joint; and 2) failure to provide adequate embedment for double-headed tension ties at the joint. The report also cited a need for the use of rational design checks for the joint. Strut-and-tie modeling would have provided a rational procedure for checking the detailing of the joint. If a strut-and-tie model had been applied to the joint, the inadequate anchorage of the double-headed tie reinforcement would have become apparent (Fig. 13(b)). Test specimens of the tricell joint revealed a mode of failure in which shear cracks in the walls of the joint bypassed the ends of the double-headed tie bars (Fig. 13(a)). In redesign details, the length of the double headed ties was increased by 500 mm, shifting the termination

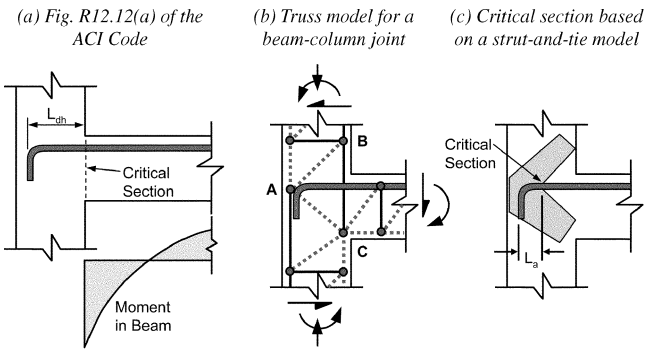

Fig. 12—Different approaches to determining critical section for bar anchorage.

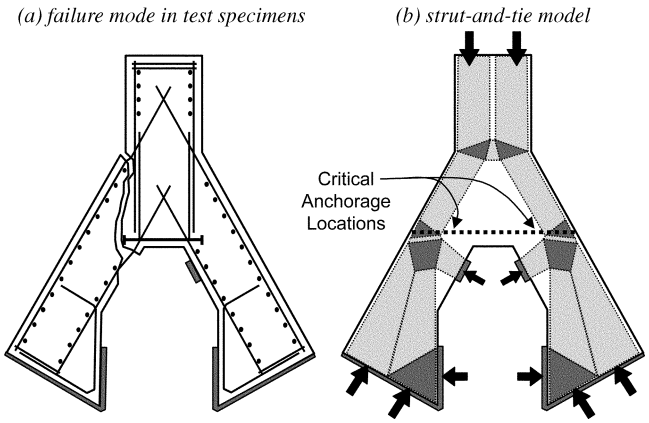

Fig. 13—Tricell joint test for Sleipner A failure investigation.

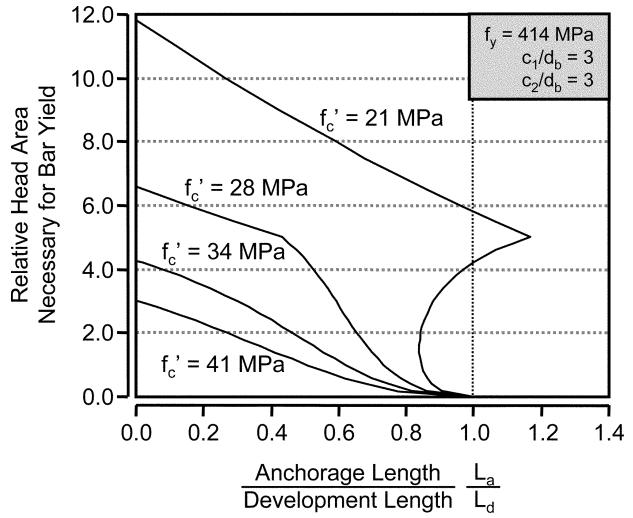

Fig. 14—Headed bar anchorage curves using proposed model.

point of the ties into the compression zone of the joint walls (additionally, much more stirrup reinforcement was provided in the region of the joint to carry recalculated shear forces). Improvements to the detailing of the joint specimens provided as much as a 70% increase in capacity.

These examples illustrate the need to use STM as a rational basis for determining anchorage length, which is distinct from embedment depth. Lessons from the Sleipner A loss particularly highlight the danger of not fully considering the flow of stress in the anchorage zone as a proper strut-and-tie model should.

While STM is the best approach for determining anchorage length, it is not yet a method that is fully understood by the engineering community, nor is it exactly clear what the best approaches are for determining appropriate node and strut dimensions for any given problem. The node and strut dimensions play a critical role in defining the anchorage length, and more development of this aspect of the STM method is necessary to fully implement the proposed model.

Use of proposed model

Total bar stress is the sum of the bar stresses provided by head bearing and bond. A designer wishing to use the model will want to answer one of two questions:

1. Given a specified head size, the designer will want to know the required anchorage length to reach yield stress in the bar, f_y.

Solution: If the head size is known, then relative head area and $f_{s,head}$ can be calculated. If $f_{s,head}$ is less than f_y, then the remaining bar stress must be carried by bond, $f_{s,bond} = f_y - f_{s,head}$. Setting $\chi \cdot f_y \cdot (L_a/L_d) = f_y - f_{s,head}$, the necessary anchorage length can be solved for. Note that in no case should L_a less than $6d_b$ be used.

2. Given a limited length over which to anchor a bar (L_a), the designer will want to know the required head size to reach yield stress in the bar.

Solution: Using the available anchorage length, the contribution from bond can be calculated (note, some allowance for the thickness of the head should be accounted for in L_a.). A trial value for the reduction factor χ must be selected initially. The bar stress required from the head is equal to $f_y - f_{s,bond}$. The required relative head area is calculated as

$$\frac{A_{nh}}{A_b} \geq \left[\frac{(f_y - f_{s,bond})}{2 \cdot n_{5\%} \cdot f_c' \cdot \Psi \cdot (c/d_b)}\right]^2 \quad (6)$$

If the trial value of χ does not correspond to the calculated relative head area, then iteration is required until χ is correctly calculated by the final A_{nh}/A_b.

Limitations of proposed model

For some situations, the proposed model will provide unrealistic combinations of relative head area and anchorage length. Curves presenting combinations of relative head area and anchorage length that provide yielding are plotted in Fig. 14 (for the case of relative cover dimensions of 3.0 and bar yield stress of 414 MPa). For $f_c' \geq 28$ MPa, the model provides reasonable curves; however, for $f_c' = 21$ MPa, the model implies that an anchorage length longer than the development length is necessary for some head sizes. This outcome results from flaws of the proposed reduction factor for bond. The reduction factor is based on a relatively small database that is not representative of the full range of the variables that may influence the behavior. Despite this flaw, the approach of the proposed model is recommended in principle; however, the need for additional study is recognized.

CONCLUSIONS

A proposed model for the anchorage capacity of headed reinforcement has been presented. The model consists of two components: 1) head bearing; and 2) bond. The bar stress provided by head bearing ($f_{s,head}$) is calculated using Eq. (3). The bar stress provided by bond ($f_{s,bond}$) is calculated using Eq. (5). Total bar stress is the sum of the two. A minimum anchorage length L_a of $6d_b$ is recommended. Strut-and-tie modeling is recommended for the calculation of anchorage length.

ACKNOWLEDGMENTS

The support of the Texas Department of Transportation and the guidance of the project supervisor D. Van Landuyt is gratefully acknowledged. The test program was conducted at the Ferguson Structural Engineering Laboratory of the University of Texas at Austin. The help of the laboratory staff and special efforts of graduate students M. Ziehl and A. Ledesma were essential to the conduct of the study.

NOTATION

A_b = bar area, mm^2
A_{gh} = gross head area, mm^2
A_{nh} = net head area, $A_{gh} - A_b$, mm^2
A_{tr} = area of confining reinforcement that ties lapped bars to compression zone, mm^2
b = minimum lateral width of strut measured perpendicular to line of force, mm
c = minimum cover dimension, measured to bar center, mm
c_2 = minimum cover dimension, measured in direction orthogonal to c, mm
d = distance from extreme compression fiber to center of longitudinal reinforcement, mm
d_b = bar diameter, mm
f_c' = concrete compression strength, from cylinder tests, MPa
f_s = bar stress, in general, MPa
$f_{s,bond}$ = bar stress provided by bond, MPa
$f_{s,head}$ = bar stress provided by head bearing, MPa
h_1 = length of strut along line of force, mm
L_a = anchorage length, measured from point at which tie bar first intersects strut boundary to end of tie bar, mm
L_s = lap splice length, measured between head faces, mm
$n_{5\%}$ = 5% fractile coefficient
P = bearing reaction at CCT node, kN
s_b = center-to-center spacing between bars in layer, mm
u_{bond} = average bond stress along bar, MPa
θ_{strut} = strut angle, measured between axis of tie bar and axis of strut
Ψ = radial disturbance factor, $0.6 + 0.4(c/c_2) \leq 2.0$

REFERENCES

1. Thompson, M. K.; Ziehl, M. J.; Jirsa, J. O.; and Breen, J. E., "CCT Nodes Anchored by Headed Bars—Part 1: Behavior of Nodes," *ACI Structural Journal*, V. 102, No. 6, Nov.-Dec. 2005, pp. 808-815.

2. Thompson, M. K.; Jirsa, J. O.; and Breen, J. E., "CCT Nodes Anchored by Headed Bars—Part 2: Capacity of Nodes," *ACI Structural Journal*, V. 103, No. 1, Jan.-Feb. 2006, pp. 65-74.

3. Thompson, M. K.; Ledesma, A.; Jirsa, J. O.; and Breen, J. E., "Lap Splices Anchored by Headed Bars," *ACI Structural Journal*, V. 103, No. 2, Mar.-Apr. 2006, pp. 271-279.

4. ACI Committee 318, "Building Code Requirements for Structural Concrete (ACI 318-02) and Commentary (318R-02)," American Concrete Institute, Farmington Hills, Mich., 2002, 443 pp.

5. DeVries, R. A., "Anchorage of Headed Reinforcement in Concrete," PhD dissertation, University of Texas at Austin, Austin, Tex., Dec. 1996, 294 pp.

6. Bashandy, T. R., "Application of Headed Bars in Concrete Members," PhD dissertation, University of Texas at Austin, Austin, Tex., Dec. 1996, 299 pp.

7. Wright, J. L., and McCabe, S. L., "The Development Length and Anchorage Behavior of Headed Reinforcing Bars," *SM Report* No. 44, University of Kansas Center for Research, Lawrence, Kans., Sept. 1997.

8. Holand, I., "The Loss of the Sleipner Condeep Platform," *DIANA Computational Mechanics '94*, Proceedings of the First International DIANA Conference on Computational Mechanics, Kluwer Academic Publishers, Dordrecht, The Netherlands, 1994, pp. 25-36.

9. Holand, I., "Sleipner A GBS Loss, Report 17: Main Report," SINTEF, *Report* No. STF22 A97861, Trondheim, Norway, 1997, 25 pp.

10. Thompson, M. K.; Jirsa, J. O.; Breen, J. E.; and Klingner, R. E., "Anchorage Behavior of Headed Reinforcement: Literature Review," *Center for Transportation Research Report* 1855-1, Austin, Tex., May 2002, 112 pp.

11. Thompson, M. K.; Young, M. J.; Jirsa, J. O.; Breen, J. E.; and Klingner, R. E., "Anchorage of Headed Reinforcement in CCT Nodes," *Center for Transportation Research Report* 1855-2, Austin, Tex., May 2002, 160 pp.

12. Thompson, M. K.; Ledesma, A. L.; Jirsa, J. O.; Breen, J. E.; and Klingner, R. E., "Anchorage of Headed Reinforcement in Lap Splices," *Center for Transportation Research Report* 1855-3, Austin, Tex., May 2002, 122 pp.